Desalination and Water Treatment
www.deswater.com

doi:10.5004/dwt.2018.22089

111 (2018) 12–21
April

Evaluation of forward osmotic backwashing of cleaning efficiency and fouling characteristics according to net driving pressure of seawater reverse osmosis (SWRO) processes

Jun Young Park[a], Ki Tae Park[b], Minjin Kim[b], Hyung Soo Kim[b], Ji Hoon Kim[b,*]

[a]*Center of Built Environment, Sungkyunkwan University, Suwon, Korea*
[b]*Graduate School of Water Resources, Sungkyunkwan University, Suwon, Korea, Tel. +82-31-290-7647, Fax +82-31-290-7549, email: jjtt23@skku.edu*

Received 20 September 2017; Accepted 10 November 2017

ABSTRACT

Contrary to general microfiltration (MF) and ultrafiltration (UF), reverse osmosis (RO) processes are affected by various osmotic pressures according to the raw water characteristics because they use semi-permeable membranes. Thus, the net driving pressure applied when operating RO processes changes. This net driving pressure greatly affects energy consumption and operating efficiency and particularly changes fouling tendencies of RO process. In this paper, seawater reverse osmosis (SWRO) processes were operated by changing the salt concentration of raw water and operating pressure to analyze the fouling characteristics at various net driving pressures. Here, the result of the experiment showed that, the flux increased with increasing net driving pressure. When fouling occurred, the operation time was reduced to a flux decline rate (FDR) of 10% according to the net driving pressure, and the accumulation of organic matter on the membrane surface increased. The fouling index increased with increasing net driving pressure, and the specific cake resistance decreased. The fouling layers formed by this decreased cake resistance were considered easy to remove for a short period by cleaning because they had a slightly loose structure. By performing forward osmotic backwashing (FOB) which is a maintenance cleaning methods for RO processes, the cleaning efficiency and organic matter removal efficiency increased in proportion to the net driving pressure. It was confirmed that the organic matter removal efficiency was higher than the cleaning efficiency because most of the fouling layers had a loose structure. In addition, the organic matter forming dense fouling layers that decreased the actual permeate flux was small. The fouling index decreased after FOB, and the specific cake resistance increased. This rendered it easier to remove fouling layers that had a loose structure and low density in FOB and to clean the fouling layers formed at high net driving pressure.

Keywords: Reverse osmosis membrane; Net driving pressure; Forward osmotic backwashing; Organic fouling; Fouling compaction

1. Introduction

Desalination is a process that removes salinity and other matters from seawater and brackish water for their use as domestic and industrial water. Desalination has also been explored as a solution to the pollution and shortage problems of the surface water of the existing representative water resource. In particular, reverse osmosis (RO) processes have realized more rapid technical achievement than other desalination technologies [1–4]. Fouling is inevitable in RO processes as a pressure-driven membrane process, and multiple fouling such as organic, inorganic, microbial, and particulate fouling occurs [5]. Such fouling increases the construction costs of desalination plants, decreases operating efficiency, and increases operating costs because of the need to apply a high safety factor [6]. Moreover, foul-

*Corresponding author.

ing causes physicochemical damage to membranes, which reduces their lifespan and causes problems such as deterioration of the quality of the produced water [7].

RO membrane fouling is highly correlated with various conditions such as raw water characteristics (i.e. water quality and water temperature) [8], RO membrane characteristics (surface charge and roughness) [9], and operating conditions of RO processes (pressure, flux, recovery rate [10], pretreatment process and treated water quality [11–13]. Among these conditions, operating pressure is an important factor because it is closely related to foulants compaction, flux, and energy consumption. According to previous studies, while high operating pressure usually increases water production by high flux, it worsens irreversible fouling [14,15]. In contrast to microfiltration (MF) and ultrafiltration (UF) processes, irreversible fouling worsens due to fouling layer compaction in RO processes operated at high pressure [16]. Furthermore, RO processes are affected by osmotic pressures according to the raw water characteristics because they use semi-permeable membranes. Thus, the net driving pressure applied when operating RO processes changes, and fouling tendencies change depending on this net driving pressure.

In general, RO processes are performed sequentially and continuously based on the chemical cleaning cycle. Thus, indirect fouling control performed before and after the occurrence of fouling [17,18]. However, because the active response of indirect fouling control during RO processes is difficult, indirect fouling eventually reduces operational efficiency. In addition, when the timing of Clean in place (CIP) is delayed, the cleaning efficiency decreases due to the deterioration of irreversible fouling, and the physicochemical damage to membranes, possibly causing secondary environmental problems [19].

Recently, studies have been carried out on maintenance cleaning as a direct fouling control method capable of relatively delaying the occurrence of irreversible fouling in RO processes. In forward osmotic backwashing (FOB), foulants swell on or detach from the membrane surface, thus removing the fouling by the shear force of circulation flow, whereby permeate water is diffused to the feed water by lowering the operating pressure in the RO processes or by using feed water with a higher osmotic pressure [20]. FOB prevents foulants from becoming irreversible by periodically removing reversible foulants on the RO membranes. Thus, it is possible to delay CIP cycles and to operate more stable RO processes [21].

In this paper, seawater reverse osmosis (SWRO) processes were operated by changing the salt concentration of raw water and operating pressure to analyze the fouling characteristics at various net driving pressures. Additionally, in this study, organic fouling of RO membrane was induced and the experimental results were analyzed using the specific cake resistance and fouling index. Furthermore, the membrane cleaning efficiency according to net driving pressure was analyzed in this study by applying FOB to fouled membranes.

2. Materials and methods

2.1. RO membrane

A commercialized 8-inch SWRO membrane made of polyamide was used in this experiment and was cut into a plate for use as a lab-scale experimental device. The cut membrane was refrigerated at 4°C by immersing in 1% sodium bisulphite solution. The SWRO membrane used in this experiment has an area of 0.0126 m^2, and a 34 mil (0.8636 mm) thick spacer was used for the feed water. The specifications of the used membrane are shown in Table 1.

2.2. Synthetic feed water

In this experiment, synthetic feed water was created and used to induce fouling. The organic matter concentration in the feed water was maintained at 100 mg/L to minimize the effects on the decrease in organic matter concentration in the feed water by the amount of organic matter accumulated on the SWRO membrane surface. Humic acid (HA) as non-biodegradable organics, sodium alginate (SA) and bovine serum albumin (BSA) were mixed at a ratio of 1:1:1 to replicate carbohydrate and protein as a typical Extracellular Polymeric Substance (EPS). The used HA, SA, and BSA were supplied by Sigma-Aldrich, and the organic matter was filtered through a 0.45 μm filter after stirring in deionized (DI) water for more than 12 h. Ca^{2+} ion was injected at 3 mM, 6 mM, and 9 mM using $CaCl_2$, and the total dissolved solids (TDS) concentration was finally adjusted to TDS 10 g/L, 20 g/L, and 30 g/L by adding NaCl.

2.3. Membrane test unit

As shown in Fig. 1, the lab-scale experimental unit used in this experiment is an exclusive RO unit capable of operating at a constant pressure with the cross-flow method for connecting two cells with a membrane area of 0.0126 m^2 in series. The concentrated waterline and permeate water line were set to repeatedly flow into the feed water tank A thermostat and stirrer were installed in the feed water tank and the NaCl solution tank so that the conditions of the feed water and NaCl solution could be constantly maintained.

The pipes were installed so that the NaCl solution instead of the feed water could be poured into the RO cells with FOB, and the brine pipes were separated so that the NaCl solution could be circulated to the NaCl solution tank. In FOB, the permeate water pipes are installed for pouring water into the RO cells using an electronic scale. Considering the changes in the efficiency of FOB due to the difference in the elevation head, the electronic scales were set at the same height as the RO cells. The electronic scales were

Table 1
Specifications of SWRO membrane

Model	SWC5
Material	Polyamide
Surface charge	Negative
Permeateflow rate (m^3/d)	34.1
Stabilizedsalt rejection (%)	99.8
Max. operatingpressure (MPa)	8.27

Note: 32,000 mg/L NaCl solution at 800 psig (5.5 MPa) applied pressure, 8% recovery, 77°F (25°C), and pH between 6.5 and 7.0.

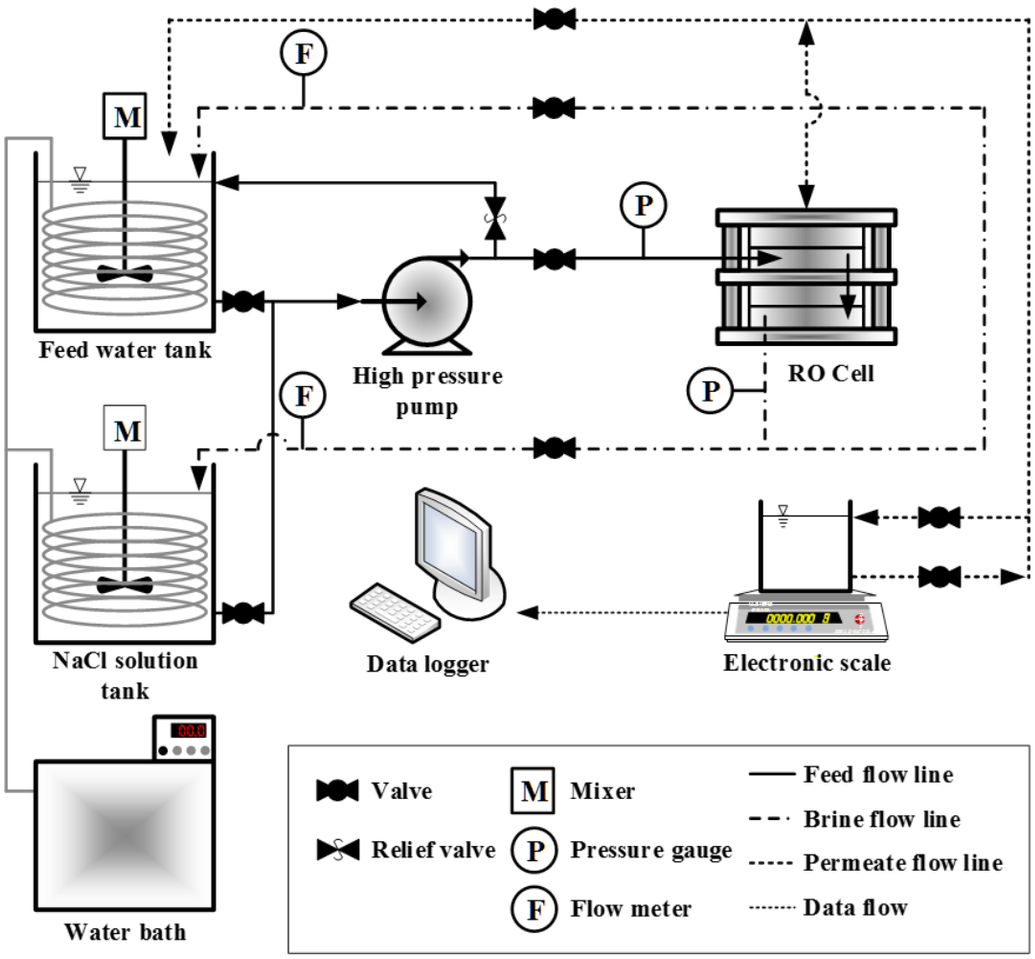

Fig. 1. Schematic diagram of experimental device for lab-scale continuous RO membrane.

connected to each RO cell to automatically measure the flux, and the pipes were installed to operate only a single RO cell in FOB.

2.4. Experimental methods

This experiment was performed with the constant-pressure control system of the cross-flow method. This experiment was also conducted at operating pressures of 30, 35, 40, and 50 bar, and FOB was performed after promoting fouling until reaching flux decline rate (FDR) of 10%. The feed water temperature was maintained at 25°C to minimize the effect on osmotic pressure and membrane permeate flux with temperature changes. Before causing fouling, the SWRO membrane was compacted at the operating pressure using deionized water for 13 h, and conditioning was then performed for two hours by adjusting the salt concentration using $CaCl_2$ and NaCl. Subsequently, fouling was induced by pouring HA, SA, and BSA at a ratio of 1:1:1 to adjust the organic matter concentration to 100 mg/L. When reaching 10% FDR, the fouling before FOB was analyzed by separating an RO cell after stopping the operation. For the remaining RO cells, the flux after FOB was measured using the feed water again after performing FOB in a NaCl solution tank for 15 min. FOB was performed to circulate NaCl solution with 35 g/L TDS by pouring it into the feed water, and the backwashing water was poured into the permeate water by maintaining its concentration at 300 mg/L TDS. The shear force was stably maintained by maintaining the circulation flow rate of 1 L/min when performing membrane filtration and FOB.

As shown in Fig. 2, the resistance after membrane compaction using the initial DI water was defined as the membrane resistance (R_m), and the increased resistance in the conditioned state after pouring the salt was defined as the salt resistance (R_{cp}). The sum of R_m and R_{cp} was the initial resistance and defined as R_i; subsequently, the resistance increased by adding organic matter and was defined as fouling resistance R_f. The membrane resistance reduced by forward osmotic backwashing was defined as reversible resistance R_r, and the membrane resistance which was not removed after forward osmotic backwashing was defined as irreversible resistance R_{ir}. R_i and R_f were defined as total resistance R_t.

The coefficient of viscosity in the fouling evaluation was determined using Eqs. (1)–(4) proposed by Sharqawy et al.

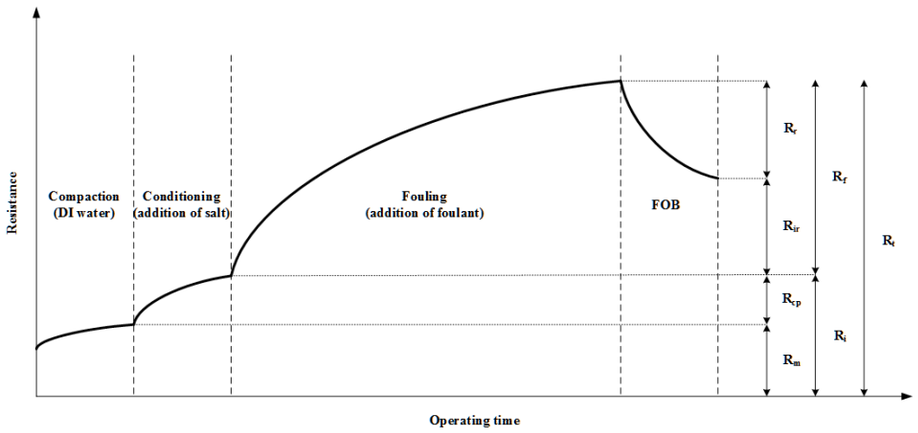

Fig. 2. Resistance classification according to experimental procedures.

[22] because it was affected by the water temperature and salinity:

$$\mu_{SW} = \mu_W(1 + A \cdot S + B \cdot S^2) \quad (1)$$

$$\mu_W = 4.2844 \times 10^{-5} + (0.157(t + 64.993)^2 - 91.296)^{-1} \quad (2)$$

$$A = 1.541 + 1.998 \times 10^{-2} t - 9.51 \times 10^{-5} t^2 \quad (3)$$

$$B = 7.974 + 7.561 \times 10^{-2} t + 4.724 \times 10^{-4} t^2 \quad (4)$$

where μ_w: viscosity coefficient of pure water, S: salinity (kg/kg), and t: water temperature (°C). The flux reduction rate associated with the constant pressure operation was calculated from Eq. (5):

$$FDR(flux\ decline\ rate) = \left(1 - \frac{j}{j_0}\right) \times 100 \quad (5)$$

where FDR: flux decline rate (%), J: reduced flux (LMH), and J_0: initial flux (LMH). After reaching 10% FDR, the cleaning efficiency was calculated from the flux recovered by forward osmotic backwashing as follows:

$$Cleaning\ efficiency = \frac{\left(J_c - J_f\right)}{\left(J_i - J_f\right)} \quad (6)$$

where J_i: initial flux (LMH), J_f: reduced flux (LMH), J_c: recovered flux after cleaning (LHM).

2.5. Extraction and analysis methods of fouling

In this experiment, organic matter was extracted by neutralizing the pH using HCl after cleaning using an ultrasonic bath at 25°C for 1 h by immersing the fouled membrane in 0.05 M NaOH solution. It is considered possible to perform an almost perfect quantitative analysis of the organic matter on the membrane surface because the cleaning efficiency was more than 99.8 ± 0.3% under these conditions, derived from the preliminary experiments in FDR 10%. The concentration of the eluted organic matter was 0.013 mg/L in the sampling experiment using virgin RO membranes and was excluded from the following experimental results. Total organic carbon (TOC) was measured using the Shimadzu TOC analyzer (TOC-L CPH), and the mean value was analyzed three times using the calibration curve of 0~15 mg/L.

3. Results and discussion

3.1. Net driving pressure and resistance by salt concentration and operating pressure

Fig. 3 shows the results of measuring the net driving pressure with changed salt concentration and the operating pressure of feed water. The net driving pressure decreased with increasing salt concentration of feed water and increased with increasing operating pressure.

Fig. 4 shows a graph of the initial resistance before injecting organic matter after conditioning according to membrane compaction and salt concentration. The membrane resistance increased in proportion to the operating pressure. This validates the assumption that an effect was only caused by membrane compaction. Salt resistance increased proportionally to operating pressure and salt concentration due to the concentration polarization and increase in membrane resistance by salt.

Rodriguez reported that membrane resistance increased with operating pressure on membranes[23], and Wang and Tarabara reported that membrane resistance increased when the filtrating solution contained only salt through the membranes [24]. This is because salt is adsorbed on membranes and the membranes swell when holding a high quantity of water. As a result, membrane resistance increases. In this study, the sum of R_m and R_{cp} is defined as the initial resistance in order to consider only the filtration resistance increased by organic matter.

3.2. Fouling characteristics according to net driving pressure

Fig. 5 shows the fouling tendency according to the TDS concentration of the feed water and operating pressure. Fouling continued until reaching 10% FDR of the timing of the general CIP to perform FOB after causing fouling. The

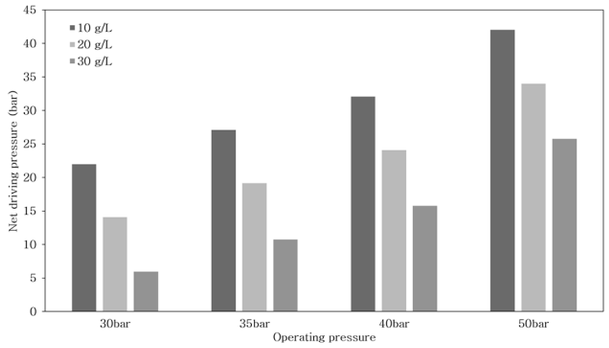

Fig. 3. Changes in net driving pressure by salt concentration of feed water and operating pressure.

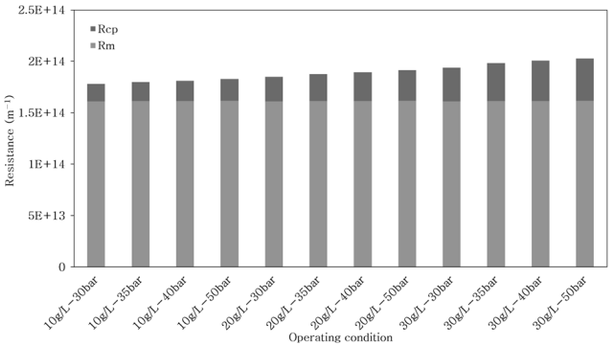

Fig. 4. Changes in initial resistance by salt concentration of feed water and operating pressure.

results of a total of four experiments are shown in the graph in Fig. 5 as the mean value and standard deviation. The result showed that, fouling worsened with increasing operating pressure at the same salt concentration of feed water. However, at the same pressure, a longer time was taken for the fouling to reach 10% FDR depending on the increase in salt concentration.

Table 2 shows a summary of the experimental results according to net driving pressure. The operating time until reaching 10% FDR decreased from 35 h at a minimum net driving pressure of 5.92 bar to 2.75 h at a maximum net driving pressure of 42 bar inversely proportional to the net driving pressure. This means that rapid fouling occurs due to high initial flux. The accumulated permeate flow rate changed from 5.39 L at a minimum net driving pressure of 5.92 bar to 2.8 L at a maximum net driving pressure of 42 bar. Although the accumulated permeate flow rate seemed to decrease according to the net driving pressure due to the limitation of 10% FDR, the permeate flow rate per unit time increased in proportion to the net driving pressure.

According to the operating condition, the amount of organic matter accumulated on the membrane surface per unit area when reaching 10% FDR showed a tendency to increase with increasing operating pressure and to decrease with increasing salt concentration of feed water. According to the net driving pressure, the amount of organic matter

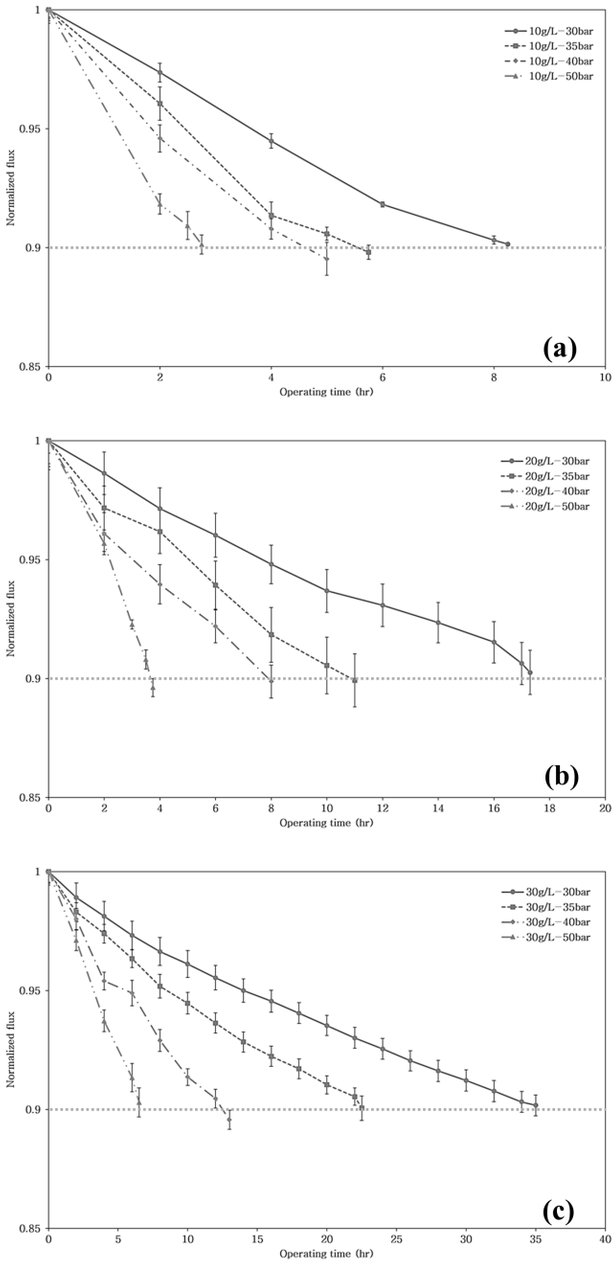

Fig. 5. Changes in membrane permeate flux according to operating pressure by salt concentration of feed water, a - TDS 10 g/L, b - TDS 20 g/L, and c - TDS 30 g/L.

increased in proportion to net driving pressure from 380.87 mg/m^2 at a minimum net driving pressure of 5.92 bar to 1,127.06 mg/m^2 at a maximum net driving pressure of 42 bar. It was clarified that the accumulation of organic matter on the membrane surface changed at the same salt concentration of feed water and fouling worsened at high membrane permeate flux. Hoek et al. published experimental results demonstrating that foulants increased on the membrane surface through the constant-pressure operation of RO processes when FDR reduced and the accumulation

Table 2
Changes in operating time, accumulated permeate water, and amount of organic matter on membrane surface according to net driving pressure

Net driving pressure (bar)	Operating pressure (bar)	Feed water TDS (g/L)	Operating time (h)	Accumulated permeate (L)	Organic mass surface density (mg/m^2)	Fouling resistance (m^{-1})	Fouling index, I (m^{-2})	Specific cake resistance before FOB, α (m/kg)
5.92	30	30	35	5.39	380.87	3.41×10^{13}	7.96×10^{13}	8.94×10^{16}
10.72	35	30	22.5	5.43	461.75	3.19×10^{13}	7.51×10^{13}	6.91×10^{16}
14.07	30	20	17.3	4.18	619.60	2.93×10^{13}	8.85×10^{13}	4.72×10^{16}
15.78	40	30	13	3.84	753.81	2.82×10^{13}	9.29×10^{13}	3.74×10^{16}
19.13	35	20	11	4.12	780.71	2.66×10^{13}	8.16×10^{13}	3.40×10^{16}
21.96	30	10	8.25	3.88	951.35	2.43×10^{13}	7.93×10^{13}	2.55×10^{16}
24.08	40	20	8	3.92	911.67	2.57×10^{13}	8.3×10^{13}	2.82×10^{16}
25.76	50	30	6.5	3.45	968.81	2.38×10^{13}	8.68×10^{13}	2.45×10^{16}
27.06	35	10	5.75	3.58	977.54	2.34×10^{13}	8.29×10^{13}	2.39×10^{16}
32.06	40	10	5	3.53	1,110.08	2.51×10^{13}	9.03×10^{13}	2.26×10^{16}
33.97	50	20	3.75	2.73	1,070.40	2.51×10^{13}	1.15×10^{14}	2.34×10^{16}
42.00	50	10	2.75	2.81	1,127.06	2.13×10^{13}	9.59×10^{13}	1.89×10^{16}

level of foulants also changed according to the gradient of FDR [25]. This makes it possible to examine the correlation between foulants on the membrane surface.

Dhananjaya stated that fouling occurs rapidly with an increase in net driving pressure but flux does not decrease at a low net driving pressure [16]. Dhananjaya also demonstrated that interactions between membrane surface and foulant required the external force to exceed the repulsive force, and that a greater force was required because the repulsive force between foulants was added to this repulsive force. However, because it was not possible to obtain a force exceeding such repulsive force at low net driving pressure, foulants were prevented from being adsorbed or accumulated on the membrane surface. As a result, a certain membrane permeate flux was maintained [16]. Charfi et al. reported that foulant accumulated on the membrane surface decreased because of shear force by the flow of feed water during cross-flow operation and showed that such a phenomenon worsened when specific cake resistance values were reduced [26]. Accordingly, the quantity of the accumulated organic matter was small under low net driving pressure due to the repulsive force between the membrane surface, organic matter, and shear force by circulation flow rate. A large amount of organic matter was accumulated even during short operating time in high flux.

The flux of the membrane processes can be expressed by the resistance in the series model based on Darcy's law [27].

$$J = \frac{\Delta P - \Delta \pi}{\mu\left(R_i + R_f\right)} \tag{7}$$

As shown in Eq. (8), R_f can be expressed by α (specific cake resistance) and I (fouling index):

$$R_f = \frac{\alpha C_b V}{A} = \frac{IV}{A} \tag{8}$$

where C_b: organic matter concentration, V: accumulated permeate volume, and A: effective membrane surface area. Based on the above description, fouling resistance can be expressed by the specific cake resistance and M (amount of organic matter accumulated on the membrane surface) as shown in Eq. (9).

$$Rf = \alpha \cdot M \tag{9}$$

The specific cake resistance shows the mass density of the fouling layer by dividing the fouling filtration resistance by the amount of organic matter accumulated on the membrane surface. This makes it possible to examine how the fouling layer is compacted. The fouling index is represented by the specific cake resistance and the organic matter concentration of the feed water, and the organic matter contained in the feed water permeated by turbulence flow due to cross-flow. The spacer on the feed water side does not accumulate on the membrane surface. Thus, as shown in Eq. (10), the fouling index was determined by deriving the relative organic matter concentration based on the amount of surface organic matter after reaching 10% FDR.

$$I = \alpha \times \frac{MA}{V} \tag{10}$$

The fouling resistance according to the operating condition when reaching 10% FDR decreased with increasing operating pressure and showed a tendency to increase with increasing salt concentration of feed water. Moreover, the resistance decreased in inverse proportion to the net driving pressure from 3.41×10^{13} m^{-1} at a minimum net driving pressure of 5.92 bar to 2.13×10^{13} m^{-1} at a maximum net driving pressure of 42 bar. The resistance produced results contrary to the amount of organic matter by net driving pressure. This is because the accumulated permeate flow rate differs due to the limitation of 10% FDR for each operating condition.

According to Rodriguez, the experiment was performed by changing the membrane permeate flux at the same accumulated permeate flow rate [23]. Thus, the operating time decreased with increasing membrane permeate flux, and the resistance increased in proportion to the membrane permeate flux [23]. However, the membrane resistance increased in proportion to the accumulated permeate flux.

Cheryan reported that most fouling models represent fouling in the form of an exponential curve according to the operating time or accumulated permeate flux [28]. A similar tendency to this was found in the results of this experiment.

The fouling indices according to the operating condition when reaching 10% FDR increased with increasing operating pressure and were not greatly affected by the salt concentration. In addition, the fouling indices increased in proportion to the net driving pressure from 7.96×10^{13} m^{-2} at a minimum net driving pressure of 5.92 bar to 9.59×10^{13} m^{-2} at a maximum net driving pressure of 42 bar. The fouling indices showed a fouling tendency of the membrane and were high as the FDR gradient decreased sharply. Sioutopoulos et al. confirmed the correlation between the FDR gradient and fouling index by transforming Darcy's law [29]. Also, Boerlage et al. reported that fouling indices increased with increasing net driving pressure in particulate fouling [30].

As a result, the specific cake resistance decreased with increasing operating pressure and increased in proportion to salt concentration. In addition, the specific cake resistance decreased inversely with the net driving pressure from 8.94×10^{16} m/kg at a minimum net driving pressure of 5.92 bar to 1.89×10^{16} m/kg at a maximum net driving pressure of 42 bar. Hong and Elimelech reported that natural organic matter (NOM) fouling layer changed to dense structure with increasing ionic strength of feed water [31]. And Li et al. confirmed that FDR decreased rapidly with increasing calcium ion and specific cake resistance increased in proportion to ionic strength [32]. The fouling index increased with increasing net driving pressure, and the specific cake resistance decreased, because a loose fouling layer was formed due to the rapidly decreasing flux. In particular, the specific cake resistance rapidly changed at a net driving pressure of 25 bar. It is necessary to consider not only the simple fouling rate but also the characteristics of fouling itself if the occurrence and recovery of fouling are considered.

3.3. Cleaning efficiency of FOB by net driving pressure

Table 3 summarizes the results of FOB after stopping fouling at 10% FDR according to net driving pressure. The cleaning efficiency increased with increasing operating pressure and showed a tendency to decrease with increasing salt concentration of feed water. Moreover, the cleaning efficiency increased in proportion to the net driving pressure from 19% at a minimum net driving pressure of 5.92 bar to 37% at a maximum net driving pressure of 42 bar.

The removal efficiency of organic matter on the membrane surface increased with increasing operating pressure and showed a tendency to decrease with increasing salt concentration of feed water. Ang et al. reported that fouling layers became denser and fouling worsened when calcium ions were combined with organic matter [33]. The results of this experiment also show that fouling occurs slowly in operations at low membrane permeate flux because the increase in salt concentration reduces the net driving pressure. However, it is considered that denser fouling occurs because the calcium ions increase in proportion to salt concentration.

Table 3
Results of FOB according to net driving pressure

Net driving pressure (bar)	Operating pressure (bar)	Feed water TDS (g/L)	Cleaning efficiency (%)	Organic removal rate (%)	FOB water volume (mL)
5.92	30	30	19	35.1	13.4
10.72	35	30	23	29.8	19.9
14.07	30	20	22	44.8	19.8
15.78	40	30	24	55.6	21.5
19.13	35	20	26	61.1	22
21.96	30	10	29	65.1	23
24.08	40	20	28	67.7	23.85
25.76	50	30	31	67.7	25
27.06	35	10	33	66.7	26
32.06	40	10	34	69.4	26
33.97	50	20	36	72	26.4
42.00	50	10	37	75.3	26.2

The organic matter removal efficiency increased in proportion to the net driving pressure from 35.1% at a minimum net driving pressure of 5.92 bar to 75.3% at a maximum net driving pressure of 42 bar. Although the cleaning efficiency and organic matter removal efficiency showed a similar tendency, the organic matter removal efficiency was relatively higher than the cleaning efficiency. This is because the compacted organic matter on the membrane in the formation of dense fouling layers causes high resistance even with a small amount of organic matter.

Jermann et al. reported the fouling tendency of HA and SA. According to the results, fouling was caused by hydrophobic interactions in HA, and reversible fouling was caused by an electrostatic repulsive force between SA molecules. When binding HA and calcium ions, HA molecules changed to a dense structure, and irreversible fouling was worsened due to mutual binding. The binding force between SA molecules was reported due to the gel layers formed when binding SA and calcium ions but binding with membranes was weak. Although HA was contained in the SA layers when binding HA and SA, HA was mainly bound on the membrane. When mixing HA and SA in calcium ion solution, HA is mixed into SA gel layers to cause more irreversible fouling [34].

The FOB water volume increased with increasing operating pressure and showed a tendency to decrease with increasing salt concentration of the feed water. In addition, the FOB water volume increased in proportion to the net driving pressure from 13.4 mL at a minimum net driving pressure of 5.92 bar to 26.2 mL at a maximum net driving pressure of 42 bar. The cleaning efficiency increased with increasing FOB water volume.

Fig. 4 shows that the resistance by salt increases with increasing operating pressure and salt concentration, and

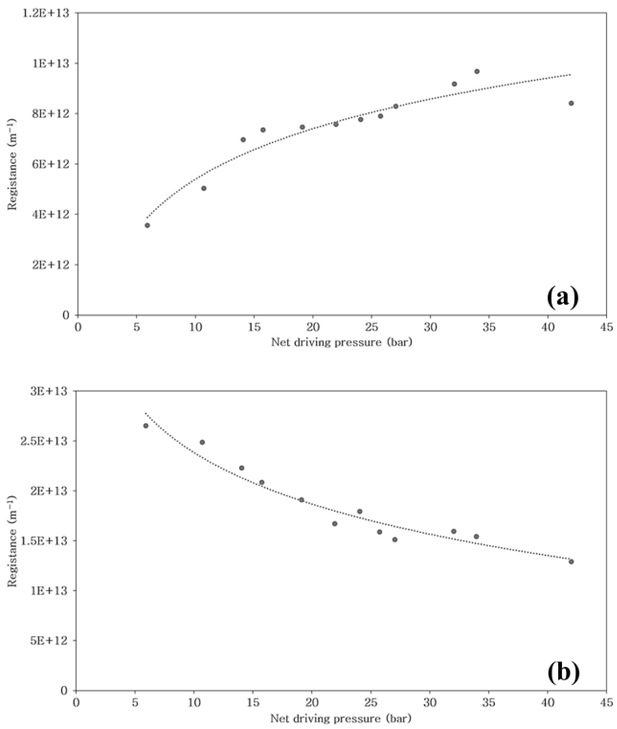

Fig. 6. Changes in resistance according to net driving pressure, a – reversible resistance, b – irreversible resistance.

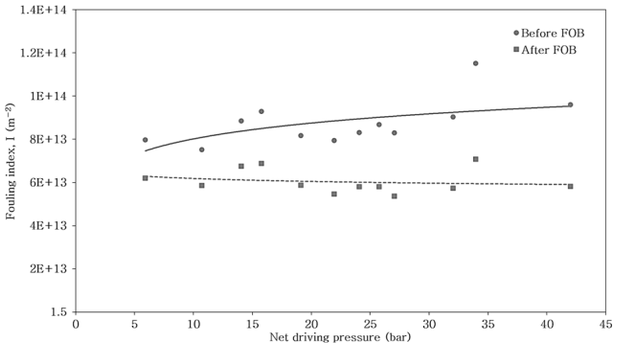

Fig. 7. Changes in fouling index according to net driving pressure before and after FOB.

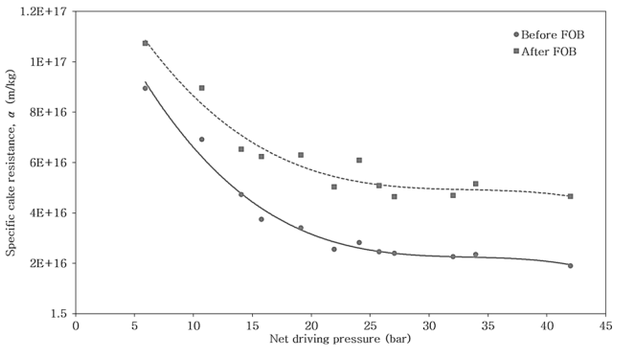

Fig. 8. Changes in specific cake resistance according to net driving pressure before and after FOB.

that the FOB water volume increases with increasing operating pressure in the FOB experiment. Sagiv et al. reported that a greater backwash flow rate was required in FOB because concentration polarization increased with increasing operating pressure due to high flux [20]. However, because resistance is relatively low at the salt concentration of the feed water (10 g/L TDS), it is considered that the salt concentration of the feed water slightly affect the inflow rate of backwashing water with an increase in net driving pressure.

The FOB water volume decreased with the increasing specific cake resistance generated before cleaning. Accordingly, the increase in the FOB water volume proportional to the increase in the net driving pressure is considered to vary according to the compaction degree of fouling. Moreover, the cleaning efficiency decreased with increasing specific cake resistance, and the organic matter removal efficiency also decreased with increasing specific cake resistance.

Fig. 6 shows the reversible and irreversible resistances according to net driving pressure. The reversible resistance increased in proportion to the net driving pressure from 3.56×10^{12} m^{-1} at a minimum net driving pressure of 5.92 bar to 8.41×10^{12} m^{-1} at a maximum net driving pressure of 42 bar. The irreversible resistance decreased in inverse proportion to the net driving pressure from 2.65×10^{13} m^{-1} at a minimum net driving pressure of 5.92 bar to 1.29×10^{13} m^{-1} at a maximum net driving pressure of 42 bar.

Fig. 7 shows the changes in the fouling index before and after FOB by net driving pressure. Although the fouling index increased according to the net driving pressure, it decreased overall after FOB. This shows that the fouling index indicating a fouling tendency was reduced by the membrane permeate flux recovered by FOB and presents only the tendency of the particular timing. Thus, it is difficult to estimate the overall operating tendency.

Fig. 8 shows the changes in the specific cake resistance before and after FOB by net driving pressure. The specific cake resistance increased after FOB, and the difference in the specific cake resistance before and after FOB is considered to be a quantitative expression according to the cleaning efficiency. Specific cake resistance is the amount of organic matter on the membrane surface and an index indicating the density of organic matter in fouling resistance. It is considered that fouling layers with low density on the feed water side were removed and then specific cake resistance values of the fouling layers with high density on the membrane surface were obtained. This made it easier to remove fouling layers with low density in FOB and confirmed the ease of cleaning the fouling layers formed at a high net driving pressure.

4. Conclusions

In this experiment, the fouling characteristics and FOB efficiency according to net driving pressure in RO processes were analyzed. As a result of the initial experiment before injecting organic matter, the net driving pressure varied depending on salt concentration and operating pressure, and the initial flux increased in proportion to the net driving

pressure. The membrane resistance increased with operating pressure, and the salt resistance increased in proportion to the operating pressure and salt concentration.

Fouling occurred until reaching 10% FDR after injecting organic matter. FDR therefore decreased rapidly with increasing operating pressure and with decreasing salt concentration. The operation time to reach 10% FDR was reduced with an increase in the net driving pressure, and the accumulated permeate flow rate also decreased. However, the accumulation of organic matter on the membrane surface increased in proportion to the net driving pressure. Although resistance decreased in inverse proportion to the net driving pressure, it increased in proportion to the accumulated permeate flow rate. It is considered that this result was obtained due to the limitation of 10% FDR. The fouling index increased with increasing net driving pressure, and the specific cake resistance decreased. The fouling layers formed by this decreased cake resistance for a short period was considered easy to remove by cleaning because the layers had a slightly loose structure.

As a result of FOB, the cleaning efficiency and organic matter removal efficiency increased in proportion to the net driving pressure. It was confirmed that the reason why the organic matter removal efficiency was higher than the cleaning efficiency was because most fouling layers had a loose structure and minimal organic matter was observed forming dense fouling layers to greatly reduce flux. In FOB, the FOB water volume showed a tendency to decrease with increasing specific cake resistance. This showed that dense fouling layers required more enhanced cleaning conditions in FOB. With an increase in the net driving pressure, the reversible resistance increased, and the irreversible resistance decreased. The fouling index decreased after FOB, and the specific cake resistance increased. This rendered it easier to the remove fouling layers that had a loose structure and low density in FOB and to clean the fouling layers formed at high net driving pressure. Based on the above results, the operation of more effective RO processes is considered possible if rapid fouling is controlled by maintenance cleaning in the operation with high flux.

Acknowledgments

This research was supported by a grant (code 17IFIP-C088924-04) from Industrial Facilities & Infrastructure Research Program funded by Ministry of Land, Infrastructure and Transport(MOLIT) of the Korea government and the Korea Agency for Infrastructure Technology Advancement (KAIA).

References

[1] M.A. Shannon, P.W. Bohn, M. Elimelech, J.G. Georgiadis, B.J. Marinas, A.M. Mayes, Science and technology for water purification in the coming decades, Nature, 452 (2008) 301–310.
[2] C. Fritzmann, J. Löwenberg, T. Wintgens, T. Melin, State-of-the-art of reverse osmosis desalination, Desalination, 216 (2007) 1–76.
[3] N. Ghaffour, T.M. Missimer, G.L. Amy, Technical review and evaluation of the economics of water desalination: Current and future challenges for better water supply sustainability, Desalination, 309 (2013) 197–207.
[4] S.R. Gray, Semiat, R, Duke, Mikel, Rahardianto, A, Cohen, Yoram Seawater use and desalination technology In: Treatise on Water Science. Wilderer, Peter A, ed Elsevier, (2011) 73–105.
[5] S. Zou, Y. Gu, D. Xiao, C.Y. Tang, The role of physical and chemical parameters on forward osmosis membrane fouling during algae separation, J. Membr. Sci., 366 (2011) 356–362.
[6] Ś.F.E. Boerlage, M.D. Kennedy, M.P. Aniye, E.M. Abogrean, G. Galjaard, J.C. Schippers, Monitoring particulate fouling in membrane systems, Desalination, 118 (1998) 131–142.
[7] B. Alley, A. Beebe, J. Rodgers, J.W. Castle, Chemical and physical characterization of produced waters from conventional and unconventional fossil fuel resources, Chemosphere, 85 (2011) 74–82.
[8] C.Y. Tang, Y.-N. Kwon, J.O. Leckie, Fouling of reverse osmosis and nanofiltration membranes by humic acid—Effects of solution composition and hydrodynamic conditions, J. Membr. Sci., 290 (2007) 86–94.
[9] M. Elimelech, Z. Xiaohua, A.E. Childress, H. Seungkwan, Role of membrane surface morphology in colloidal fouling of cellulose acetate and composite aromatic polyamide reverse osmosis membranes, J. Membr. Sci., 127 (1997) 101–109.
[10] L. Paugam, S. Taha, G. Dorange, P. Jaouen, F. Quéméneur, Mechanism of nitrate ions transfer in nanofiltration depending on pressure, pH, concentration and medium composition, J. Membr. Sci., 231 (2004) 37–46.
[11] Y.-J. Tan, L.-J. Sun, B.-T. Li, X.-H. Zhao, T. Yu, N. Ikuno, K. Ishii, H.-Y. Hu, Fouling characteristics and fouling control of reverse osmosis membranes for desalination of dyeing wastewater with high chemical oxygen demand, Desalination, 419 (2017) 1–7.
[12] M.T. Khan, C.-L.d.O. Manes, C. Aubry, J.-P. Croué, Source water quality shaping different fouling scenarios in a full-scale desalination plant at the Red Sea, Water Res., 47 (2013) 558–568.
[13] S. Mattaraj, W. Phimpha, P. Hongthong, R. Jiraratananon, Effect of operating conditions and solution chemistry on model parameters in crossflow reverse osmosis of natural organic matter, Desalination, 253 (2010) 38–45.
[14] S. Lee, C. Boo, M. Elimelech, S. Hong, Comparison of fouling behavior in forward osmosis (FO) and reverse osmosis (RO), J. Membr. Sci., 365 (2010) 34–39.
[15] J.M. Ochando-Pulido, S. Rodriguez-Vives, G. Hodaifa, A. Martinez-Ferez, Impacts of operating conditions on reverse osmosis performance of pretreated olive mill wastewater, Water Res., 46 (2012) 4621–4632.
[16] D.P. Niriella, Investigating the fouling behavior of reverse osmosis membranes under different operating conditions, 2006.
[17] W. Arras, N. Ghaffour, A. Hamou, Performance evaluation of BWRO desalination plant — A case study, Desalination, 235 (2009) 170–178.
[18] J.P. Chen, S.L. Kim, Y.P. Ting, Optimization of membrane physical and chemical cleaning by a statistically designed approach, J. Membr. Sci., 219 (2003) 27–45.
[19] J.W. Nam, J.Y. Park, J.H. Kim, Y.S. Lee, E.J. Lee, M.J. Jeon, H.S. Kim, A. Jang, Effect on backwash cleaning efficiency with TDS concentrations of circulated water and backwashing water in SWRO membrane, Desal. Water Treat., 43 (2012) 124–130.
[20] A. Sagiv, N. Avraham, C.G. Dosoretz, R. Semiat, Osmotic backwash mechanism of reverse osmosis membranes, J. Membr. Sci., 322 (2008) 225–233.
[21] M.K. Junyoung Park, Kitae Park, Hyungsoo Kim, Hyungsook Kim, Jihoon Kim Effects of cleaning conditions of osmotic backwashing on the SWRO operation, Desal. Water Treat., 77 (2017) 171–176.
[22] M.H. Sharqawy, J.H. Lienhard, S.M. Zubair, Thermophysical properties of seawater: a review of existing correlations and data, Desal. Water Treat., 16 (2010) 354–380.
[23] S.G.S. Rodriguez, Particulate and Organic Matter Fouling of Seawater Reverse Osmosis Systems: Characterization, Modelling and Applications. UNESCO-IHE PhD Thesis, CRC Press, 2011.

[24] F. Wang, V.V. Tarabara, Coupled effects of colloidal deposition and salt concentration polarization on reverse osmosis membrane performance, J. Membr. Sci., 293 (2007) 111–123.
[25] E.M. Hoek, A.S. Kim, M. Elimelech, Influence of crossflow membrane filter geometry and shear rate on colloidal fouling in reverse osmosis and nanofiltration separations, Environ. Eng. Sci., 19 (2002) 357–372.
[26] A. Charfi, J. Harmand, N.B. Amar, A. Grasmick, M. Héran, Deposit membrane fouling: influence of specific cake layer resistance and tangential shear stresses, Water Sci. Technol., 70 (2014) 40–46.
[27] G. Belfort, R.H. Davis, A.L. Zydney, The behavior of suspensions and macromolecular solutions in crossflow microfiltration, J. Membr. Sci., 96 (1994) 1–58.
[28] M. Cheryan, Ultrafiltration and microfiltration handbook, CRC press, 1998.
[29] D. Sioutopoulos, A. Karabelas, S. Yiantsios, Organic fouling of RO membranes: Investigating the correlation of RO and UF fouling resistances for predictive purposes, Desalination, 261 (2010) 272–283.
[30] Ś.F. Boerlage, M.D. Kennedy, M.P. Aniye, E.M. Abogrean, G. Galjaard, J.C. Schippers, Monitoring particulate fouling in membrane systems, Desalination, 118 (1998) 131–142.
[31] S. Hong, M. Elimelech, Chemical and physical aspects of natural organic matter (NOM) fouling of nanofiltration membranes, J. Membr. Sci., 132 (1997) 159–181.
[32] H. Li, Y. Lin, Y. Luo, P. Yu, L. Hou, Relating organic fouling of reverse osmosis membranes to adsorption during the reclamation of secondary effluents containing methylene blue and rhodamine B, J. Hazard. Mater., 192 (2011) 490–499.
[33] W.S. Ang, A. Tiraferri, K.L. Chen, M. Elimelech, Fouling and cleaning of RO membranes fouled by mixtures of organic foulants simulating wastewater effluent, J. Membr. Sci., 376 (2011) 196–206.
[34] D. Jermann, W. Pronk, S. Meylan, M. Boller, Interplay of different NOM fouling mechanisms during ultrafiltration for drinking water production, Water Res., 41 (2007) 1713–1722.